

RSC Advances



This is an *Accepted Manuscript*, which has been through the Royal Society of Chemistry peer review process and has been accepted for publication.

Accepted Manuscripts are published online shortly after acceptance, before technical editing, formatting and proof reading. Using this free service, authors can make their results available to the community, in citable form, before we publish the edited article. This *Accepted Manuscript* will be replaced by the edited, formatted and paginated article as soon as this is available.

You can find more information about *Accepted Manuscripts* in the [Information for Authors](#).

Please note that technical editing may introduce minor changes to the text and/or graphics, which may alter content. The journal's standard [Terms & Conditions](#) and the [Ethical guidelines](#) still apply. In no event shall the Royal Society of Chemistry be held responsible for any errors or omissions in this *Accepted Manuscript* or any consequences arising from the use of any information it contains.

Environmentally friendly solution route to kesterite

$\text{Cu}_2\text{ZnSn}(\text{S},\text{Se})_4$ thin films for solar cell applications

Zhenggang Li^{a,b}, John C. W. Ho^{a,b}, Kian Keat Lee^b, Xin Zeng^{a,b}, Tianliang Zhang^b,

Lydia Helena Wong^{a,b}, Yeng Ming Lam^{a,b,c,*}

^a School of Materials Science and Engineering, Nanyang Technological University, Blk N4.1, Nanyang Avenue, Singapore 639798.

^b Energy Research Institute @ NTU (ERI@N), Research Technoplaza Level 5, Nanyang Drive, Singapore 637553.

^c Institute of Materials for Electronic Engineering II, RWTH-Aachen, Sommerfeldstr. 24, D-52074 Aachen, Germany.

Abstract

Quaternary kesterite $\text{Cu}_2\text{ZnSnS}_4$ (CZTS) and $\text{Cu}_2\text{ZnSn}(\text{S},\text{Se})_4$ (CZTSSe) thin films have been prepared from a mixture of CuS, ZnS and SnS_2 nanoparticles and solar cells were made from the CZTSSe films. The binary sulfide nanoparticles were pre-synthesized in aqueous solution and then spray deposited onto glass substrates. The nano-sized binary sulfide nanoparticles have a large surface area that provides the driving force for solid-state reactions between the nanoparticles and results in the formation of the quaternary CZTS phase at moderate temperatures. The CZTSSe solar cells were prepared using the binary sulfide nanoparticles films annealed in Se vapor and the cells showed an encouraging efficiency of 5.12% ($V_{oc} = 378$ mV, $J_{sc} = 26.2$ mA/cm² and FF = 51.7%). Our synthetic approach provides a low-cost, environmentally friendly and easy to scale up option for the preparation of CZTSSe thin films for solar cell applications.

* Author to whom correspondence should be addressed. Electronic mail:

ymlam@ntu.edu.sg

1. Introduction

Quaternary chalcogenide $\text{Cu}_2\text{ZnSnS}_4$ (CZTS) is an absorber material suitable for use in thin film solar cells because it has a direct band gap around 1.5 eV, it has a large absorption coefficient of around 10^4 cm^{-1} and it is made up of abundant elements.¹⁻⁴ To date, several routes have been developed to deposit CZTS thin films.⁵ Vacuum-based deposition techniques have been very successful in demonstrating high efficiencies in CIGS solar cells and therefore have been widely adopted in the deposition of CZTS thin films.^{6, 7} Katagiri and co-workers pioneered the early studies of CZTS solar cells.^{1,8,9} With radio frequency (RF) co-sputtering of elemental and binary sulfide precursors, they were able to achieve a solar cell efficiency of 6.77%.¹⁰ In another popular approach, Cu-, Zn- and Sn-metal layers are deposited by sputtering, then the films are annealed at high temperature in an H_2S environment to form CZTS.¹¹ The Cu : Zn : Sn ratio can be controlled by varying the thickness of each metal layer. More recently, Shin et al. made use of co-evaporation of Cu, Zn, Sn and S followed by annealing to obtain a device with a high efficiency of 8.4% from a device area of 0.45 cm^2 .¹² Despite the excellent progress, vacuum-based techniques still require a high energy input and impose a significant cost on devices. Hence, there is a move towards finding an alternative low-cost fabrication method to the vacuum deposition techniques.

In recent years, there is an increasing amount of work done on the deposition of CZTS thin films using low-cost solution-based methods. Scragg et al. fabricated CZTS thin film

solar cells using electrodeposited stacked metal layers and was able to achieve an efficiency of 3.2%.¹³ Kumar et al. synthesized CZTS thin films by spray pyrolysis, where the precursor solution contained Cu-, Zn-, Sn-salts and thiourea.^{14, 15} The CZTS nanoparticle approach and hybrid solution-particle approach have attracted more interest than other methods due to the possibility of generating solar cells with a high power conversion efficiency - 7.2% for the nanoparticle method and beyond 12.0% for the solution method.^{16, 17} For the CZTS nanoparticle approach, the CZTS nanocrystals have often been synthesized using the hot coordinating solvent method and the nanocrystals then deposited on the substrate and annealed to form the absorber layer.¹⁸⁻²² The hybrid solution-particles approach made use of a slurry containing Cu- and Sn-chalcogenide solution precursors and Zn-chalcogenide nanoparticles dispersed in hydrazine (N₂H₄), which was then spin-coated and annealed to form the CZTS layer.²³

To date, it has been shown that solution processed CZTS solar cells have a reasonably high conversion efficiency and hence considering both device performance and cost, there is potential for this technology to compete with the more mature CdTe and CIGS technologies. The chemicals involved as well as the by-products of the synthesis process have low toxicity which is an added advantage. Since CZTS can be processed in solution, the fabrication process can be easily scaled up for mass production.

There are disadvantages associated with some of the solution deposition processes. Compared to the other solution deposition methods, the electrodeposition method suffers from low conversion efficiency. For the spray pyrolysis method, the NH₃ and HCl byproducts generated suggest that this method is less environmentally friendly, especially for large quantity production.^{24, 25} Although the CZTS nanoparticle approach and hybrid

solution-particle approach were able to produce high efficiency solar cells, both methods have issues that limit large scale practical applications: (i) the use of expensive and toxic organic solvents (oleylamine, hexadecylamine for the former, and hydrazine for the latter) that may increase the fabrication cost and also lead to environmental issues; (ii) highly demanding processing conditions such as high reaction temperature and inert environment make the processes difficult to scale up. Therefore, a novel synthesis method that is cost-effective, environmentally benign and easily up-scalable is required.

Here, we report one such method for the preparation of CZTS thin films. Since $\text{Cu}_2\text{ZnSnS}_4$ is a quaternary compound, instead of using ionic compounds as the precursors, a combination of CuS, ZnS and SnS_2 binary sulfide in the ratio 2:1:1 can be transformed into quaternary films via solid state reactions. These binary sulfide nanoparticles can be easily synthesized in an aqueous environment. This method allows the use of the most common Cu-, Zn- and Sn-precursors including chlorides, sulfates, nitrates and acetates, while the sulfur source is from hydrated sodium sulfide ($\text{Na}_2\text{S}\cdot 9\text{H}_2\text{O}$). The deposition techniques for these solutions could then be spray coating, printing, spin-coating, and many other solution deposition techniques. This route could allow easy tuning of the composition of the films and the possibility of preparing stable inks for printing. Hence, this work paves the way for a large scale and environmentally friendly way to fabricate thin film solar cells.

2. Experimental

Materials

Copper (II) acetate ($\text{Cu}(\text{OAc})_2$, Aldrich, 98%), zinc acetate ($\text{Zn}(\text{OAc})_2$, Aldrich, 99.99%), tin (IV) chloride pentahydrate ($\text{SnCl}_4\cdot 5\text{H}_2\text{O}$, Sigma-Aldrich, 98%), sodium sulfide

nonahydrate ($\text{Na}_2\text{S}\cdot 9\text{H}_2\text{O}$, Aldrich, 98%), (n-hexadecyl) trimethyl ammonium bromide (CTAB, Lancaster, 98%) and ethanol (Aik Moh Paints & Chemicals, 95%) were purchased and used as received. Milli-Q water (Millipore, $18.5 \text{ M}\Omega\text{cm}$ at $25 \text{ }^\circ\text{C}$) was used in all synthesis and subsequent preparation steps.

Synthesis of binary sulfide nanoparticles

The preparation of CZTS films consists of four consecutive steps as shown in Fig.1: (i) synthesis of CuS, ZnS and SnS_2 nanoparticles, (ii) mix the sulfide nanoparticles in the desired molar ratio in either water or ethanol to form the nanoparticle precursor solution, (iii) deposit the precursor solution onto substrates to form precursor films and (iv) anneal the precursor films to form CZTS films. The CuS, ZnS and SnS_2 nanoparticles were synthesized using precipitate reactions between S^{2-} anions and Cu^{2+} , Zn^{2+} or Sn^{4+} cations in aqueous solution respectively. (n-hexadecyl) cetyl trimethylammonium bromide (CTAB) was used as the capping ligand for all three types of nanoparticles. During the experiment, freshly prepared sulfur precursor solution was added to the cation precursor solutions drop by drop with constant stirring at room temperature ($25 \text{ }^\circ\text{C}$). The solution was allowed to react for some time. After synthesis, the CuS, ZnS and SnS_2 nanoparticles were washed and cleaned thoroughly using water and ethanol and then centrifuged. The as-prepared CuS, ZnS and SnS_2 nanoparticles can be re-dispersed in water or ethanol.

Preparation of CZTS and CZTSSe thin films

In a typical experiment, 95.6 mg CuS (1 mmol), 48.7 mg ZnS (0.5 mmol) and 91.4 mg SnS_2 (0.5 mmol) were weighed and added to 300 ml of ethanol. This solution was then ultrasonicated for 30 min followed by another 30 min of stirring in order to form a well-

dispersed precursor solution. Subsequently, the precursor solution was spray deposited onto sodium lime glass (SLG) substrates to form precursor films. During the spraying process, the SLG substrates were heated to 100 °C in air to remove most of the solvent. Finally, the precursor films were annealed for 30 min under an Ar gas environment at temperatures of 200 °C, 300 °C, 400 °C and 450 °C. The $\text{Cu}_2\text{ZnSn}(\text{S}, \text{Se})_4$ (CZTSSe) thin films were prepared by annealing the precursor CZTS films under Se vapor with As gas as the background gas at 520 °C for 12 min.

Preparation of CZTSSe thin film solar cells

The photovoltaic devices were fabricated using the following standard procedure – CZTSSe thin films were deposited and selenized on molybdenum on glass then 50 nm CdS was deposited using chemical bath deposition. 50 nm of i-ZnO was then deposited using DC sputtering followed by 400 nm ITO deposited using RF sputtering. Lastly, a patterned Au grid was thermally evaporated as the top electrode.

Characterization

The grazing incidence x-ray diffraction (GIXRD) patterns were obtained using a Bruker D8 Advance equipped with Cu $K\alpha$ radiation ($\lambda = 1.54 \text{ \AA}$). The Raman analysis was performed using a Renishaw inVia Raman microscope with a 488 nm laser. Scanning electron microscopy (SEM) images were acquired using a JEOL JSM 7600F FESEM operating at an accelerating voltage of 5 kV. The SEM is equipped with an Oxford X-MAX EDS detector, which was used to estimate the atomic ratio of Cu, Zn, Sn and S. An accelerating voltage of 20 kV was used for the EDS measurements. The TEM analysis was performed using a JEOL 2100F field emission microscope operating at an

accelerating voltage of 200 kV. Current density-voltage (J-V) characteristics of the CZTSSe devices were obtained with an AM1.5G solar simulator (VS-0852) equipped with a 500 W xenon lamp and a Keithley sourcemeter (2612A, dual sourcemeter, 200V). The light intensity of the solar simulator was calibrated with a Si photodiode (Fraunhofer) to 100 mW/cm². The quantum efficiency measurement was carried out with a PVE300 Photovoltaic Devices Characterisation System (Bentham) equipped with a xenon/quartz halogen light source and calibrated with Si/Ge reference detectors.

3. Results and discussion

CZTS Thin Films The as-synthesized CuS, ZnS and SnS₂ nanoparticles can be easily dispersed in either water or ethanol. Fig. 2 shows TEM images of the CuS, ZnS and SnS₂ nanoparticles. XRD patterns from the CuS, ZnS and SnS₂ nanoparticles are shown in the Supporting Information, Fig. S1. The size of all three types of nanoparticles is found to be in the order of tens of nanometers. These small particles have a very larger surface energy compared to micron-sized particles and this means that there is a strong driving force for coalescence driven by a reduction in surface energy. Another advantage of nanoparticles over micron sized or larger particles is that these smaller sized particles can be packed closer to each other and therefore during annealing, the Cu, Zn, Sn and S atoms only need to diffuse a short distance to their nearest neighbors during the transformation from binary nanoparticles to a CZTS film. The size dispersion of all the binary nanoparticles remains stable with no obvious aggregation for up to three hours. Any localized agglomeration of the same species may lead to non-uniformity in the composition of the final CZTS thin film. Recently, Cao et al. demonstrated high efficiency CZTSSe solar cells making use of binary and ternary sulfide nanoparticles.²⁶

However, in their work, organic solvents including oleylamine and trioctylphosphine oxide were still involved in the synthesis of these nanoparticles. Woo et al. prepared CZTS films with a powder mixture of binary sulfide and elemental precursors.²⁷ Despite the use of non-toxic ethanol as the solvent, this method is not ideal as the precursor powders were milled to grind them down to finer dimensions and generally milling will tend to result in relative large precursor particles as well as non-uniform distribution of the Cu, Zn, Sn and S precursors.

Ethanol was used as a solvent in the synthesis of the CZTS thin film because its boiling point is low compared to water thus allowing for a low substrate temperature during the spray process (~ 100 °C), minimizing possible oxidation issues. A mixture of CuS, ZnS and SnS₂ nanoparticles (molar ratio 2:1:1) in ethanol was sprayed onto glass substrates and the precursor films were annealed at different temperatures – 200, 300, 400 and 450 °C for 30 min under Ar gas. As shown in Fig. 3, the XRD pattern of the as-deposited precursor film is a composite of the XRD patterns of the CuS, ZnS and SnS₂ nanoparticles. After annealing at 200 °C for 30 min, the 2θ peaks at 29.3°, 31.8°, 32.9°, 47.9°, 52.7° and 58.7° became sharper compared to the as deposited precursor film, indicating an increase in the crystallinity of the CuS nanoparticles. Sharp peaks at 28.5°, 47.3° and 56.2° can be observed for samples annealed at 300, 400 and 450 °C, which correspond to the (112), (220) and (312) planes of kesterite CZTS (JCPDS no. 26-0575). In addition to the three major peaks, minor peaks at 18.2°, 23.1°, 33.0°, 69.3° and 76.5° could also be observed for samples annealed at 400 and 450 °C. Therefore, both the major and minor peaks indicate that the CZTS phase has been formed. Comparing the XRD patterns of the films annealed at various temperatures, the full width at half maximum

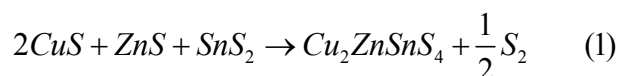
(FWHM) for the (112) peak is found to decrease as the annealing temperature increases from 300 to 450 °C, which indicates that the average CZTS crystallite size in the annealed film increases with annealing temperature.

From the previous discussion, it is evident that the kesterite CZTS phase was formed at temperatures higher than 300 °C. Unfortunately, some binary and ternary phases, Cu₂S (JCPDS no. 4-15-2234), ZnS (JCPDS no. 5-0566) and Cu₂SnS₃ (JCPDS no. 1-089-4714), also share a similar crystal structure, which makes it difficult to conclusively demonstrate the formation of pure CZTS using only XRD data. Raman spectra provide information on the vibrational properties of crystalline samples and are therefore useful for determining the presence of binary and ternary phases in thin films. This technique has been well-established for the identification of impurity phases in CZTS films.^{28,29} The Raman peaks for CZTS (288, 338 and 368 cm⁻¹), Cu₂S (475 cm⁻¹), ZnS (278 and 351 cm⁻¹) and Cu₂SnS₃ (298 and 356 cm⁻¹) are distinct.³⁰⁻³³ Hence, in order to confirm the phase purity, Raman analysis was performed. As shown in Fig. 4, samples annealed at all three temperatures exhibit a strong peak at 336 cm⁻¹ with two weaker shoulder peaks at 288 and 368 cm⁻¹. The above three peaks are indicative of the presence of the CZTS phase in the films annealed at 300, 400 and 450 °C. The strong peak at 336 cm⁻¹ corresponds to the symmetric A mode vibration.³⁴ In addition, within the resolution of the Raman measurement, no noticeable peaks corresponding to Cu₂S (475 cm⁻¹), ZnS (278 and 351 cm⁻¹) or Cu₂SnS₃ (298 and 356 cm⁻¹) could be observed, which excludes the existence of all three possible impurity phases. Raman analysis thus confirms that pure CZTS films were formed at temperatures higher than 300 °C.

The grain size of the CZTS films is important in determining the performance of the solar

cells. In CZTS based thin film solar cells, a large CZTS grain size is favored due to improved charge transport properties as compared to small grain sized films. When annealed at higher temperatures (400 °C), the grain size of the CZTS thin film can reach an average of around 100 nm (Fig. 5a) for a film that is about 1 µm thick (Fig. 5b).

As the absorption and electrical properties are determined by the composition of the film, it is important to determine the relative elemental composition. The Cu: Zn: Sn: S elemental ratio was determined to be 1.9: 0.9: 0.9: 4.2 for the precursor film using SEM energy-dispersive X-ray spectroscopy (EDS), which is in agreement with the amount of CuS, ZnS and SnS₂ added initially. This is close to the starting ratio but slightly rich in S, because the binary sulfide precursors contain excess S due to the oxidation states of the Cu binary compound. After annealing at 400 °C for 30 min, the CZTS films has a Cu: Zn: Sn: S ratio of 1.9: 1.0: 0.9: 4.1, similar to the as-deposited composition. The chemical reaction for the formation of CZTS is proposed to be



Sulfur vapor is formed as a by-product of the reaction. This creates a S-rich environment within the CZTS film, which reduces the need for a sulfurization or selenization process. Generally, CZTS films suffer from loss of Sn and S during annealing.³⁵ From the EDS data, the Sn content in the annealed CZTS films was found to remain fairly constant compared to the precursor film with only a slight S loss. This is mainly due to the relatively low annealing temperature of 400 °C.

CZTSSe Thin Films and Solar Cells Large grains are desirable for good thin film solar cells performance. Although using ethanol as the solvent, pure CZTS films have been

shown to be successfully prepared, the films is highly porous. In order to encourage grain growth, the substrate temperatures should be higher. At higher temperatures, such as 300 °C, the nanoparticle precursors can fuse and grow more, resulting in denser films. Unfortunately, it is very difficult to spray deposit the nanoparticles using ethanol as the solvent at such high temperatures because the solvent is highly flammable. Therefore, water was used as the solvent for high temperature deposition. In order to prevent the oxidation of binary sulfide nanoparticles at such high temperatures, thiourea (TU) was used as an additional sulfur precursor since it also acts as a reducing agent.

For the application in thin film solar cells, the as deposited binary sulfide particles films were thermally annealed at 500 °C for 30 min in an Ar environment after deposition to encourage the inter-diffusion of the elements resulting in the formation of CZTS films. Annealing at this high temperature will allow faster diffusion of the elements and some grain growth To encourage further grain growth, the film was then selenized at 520 °C for 12 min in selenium vapor. Fig. 6a shows XRD patterns from the annealed film and the selenized film. The XRD pattern from the annealed film matches the kesterite CZTS phase with characteristic 2θ angles of 28.5°, 47.3° and 56.2°. The XRD peaks from the selenized film are shifted to lower 2θ values as compared with the annealed film. The major peak at 28.5° for the CZTS film is shifted by 1° to 27.5° for the CZTSSe film. This is because the smaller sized S atoms are replaced by the larger Se atoms during the selenization process, resulting in larger lattice spacings for CZTSSe than for CZTS.

Solar cells were fabricated using the selenized film with a Cu-poor and Zn-rich composition. The composition used was $\text{Cu}/(\text{Zn} + \text{Sn}) = 0.72$ and $\text{Zn}/\text{Sn} = 1.2$. The $\text{Se}/(\text{S}+\text{Se})$ ratio determined by EDX was found to be approximately 0.8. Fig. 7a shows

the cross-section of a typical as-prepared CZTSSe solar cell with the configuration - Mo/CZTSSe/CdS/ZnO/ITO/Au. The size of the CZTSSe solar cells (0.11 cm^2) were defined by the Au electrode deposition. The current density–voltage (J–V) characteristics for a typical as-prepared CZTSSe solar cell measured in the dark and under AM1.5G illumination are shown in Fig. 7b. The device demonstrates a power conversion efficiency of 5.12% with an open-circuit voltage (V_{oc}) of 378 mV, a short-circuit current density (J_{sc}) of 26.2 mA/cm^2 and a fill factor (FF) of 51.7%. The series resistance (R_s) and shunt resistance (R_{sh}) are determined to be $3.6 \Omega \cdot \text{cm}^2$ and $404 \Omega \cdot \text{cm}^2$ respectively. The device performance is comparable with some of the best performing nanoparticle based CZTSSe solar cells, showing that our approach is highly promising for CZTSSe based solar cells.^{16,26,27} The thickness of our absorber film was around 800 nm and the grain size less than 500 nm, both of which are well below that for optimum CZTSSe device performance.²³ Further optimization could be made by increasing the thickness of the CZTSSe film, which would certainly lead to an improvement in J_{sc} and hence the efficiency of the solar cell. On top of this, by modifying the film composition as well as the selenization processes, the grain size can be increased and this will lead to an increased photocurrent generation and a reduction in recombination.

Fig. 8 shows the external quantum efficiency (EQE) of the CZTSSe based solar cell as a function of photon wavelength. The EQE is fairly high (more than 60%) between 500 to 900 nm. The band gap of the absorber layer is determined to be 1.18 eV by fitting a plot of $[\text{h}\nu \ln(1-\text{EQE})]^2$ vs. $\text{h}\nu$ near the band edge (Inset of Fig. 8). Our calculated band gap matches well with the reported range of 1.0 eV to 1.5 eV for CZTSSe using EQE measurements.³⁶ It is also in good agreement with the band gap of CZTSSe based on

optical absorption measurements.³⁷ The band gap estimate based on EQE is reasonable considering the majority of S atoms are replaced with Se during the selenization process.

4. Conclusion

In conclusion, we have developed a low-cost, environmentally friendly and easily up-scalable method to prepare CZTS thin films by making use of aqueous solution synthesized CuS, ZnS and SnS₂ nanoparticles. Post-annealing plays an important role in the phase evolution from binary phases to the quaternary CZTS phase. The as-prepared CZTS films were S rich due to the excess sulfur content associated with the binary sulfide phases. CZTSSe thin film solar cells with the following architecture: Mo/CZTSSe/CdS/ZnO/ITO/Au were fabricated. The as-fabricated device exhibited a total area efficiency of 5.12% with V_{oc} of 378 mV, J_{sc} of 26.2 mA/cm² and FF of 51.7%. These results are comparable with some of the best performing nanoparticle based CZTSSe solar cells.

Acknowledgments

This project is supported by the Singapore NRF-CRP grant “Nanonets for harnessing solar energy and storage”. YML acknowledges support from the Danish Council for Strategic Research under the CHASOL project. LHW acknowledges support from National Research Foundation (NRF), Prime Minister’s Office, Singapore under its Campus for Research Excellence and Technological Enterprise (CREATE) program and A*STAR SERC Printed Photovoltaic Program Grant (1021700143). The authors will like to acknowledge Dr C. Boothroyd for proof reading the manuscript.

References

- 1 Katagiri, H. *Thin Solid Films* **2005**, 480-481, 426- 432.
- 2 Seol, J. S.; Lee, S. Y.; Lee, J. C.; Nam, H. D.; Kim, K. H. *Sol. Energ. Mater. Sol. Cells* **2003**, 75, 155-162.
- 3 Andersson, B. A. *Prog. Photovoltaics* **2000**, 8, 61-76.
- 4 Wadia, C.; Alivisatos, A. P.; Kammen, D. M. *Environ. Sci. Technol.* **2009**, 43, 2072-2077.
- 5 Mitzi, D. B.; Gunawan, O.; Todorov, T. K.; Wang, K.; Guha, S. *Sol. Energ. Mater. Sol. Cells* **2011**, 95, 1421- 1436.
- 6 Repins, I.; Contreras, M. A.; Egaas, B.; DeHart, C.; Scharf, J.; Perkins, C. L.; To, B.; Noufi, R. *Prog. Photovoltaics* **2008**, 16, 235- 239.
- 7 Jackson, P.; Hariskos, D.; Lotter, E.; Paetel, S.; Wuerz, R.; Menner, R.; Wischmann, W.; Powalla, M. *Prog. Photovoltaics* **2011**, 19, 894- 897.
- 8 Katagiri, K., Sasaguchi, N.; Hando, S.; Hoshino, S.; Ohashi, J.; Yokota, T. *Sol. Energ. Mater. Sol. Cells* **1997**, 49, 407- 414.
- 9 Jimbo, K.; Kimura, R.; Kamimura, T.; Yamada, S.; Maw, W. S.; Araki, H.; Oishi, K.; Katagiri, H. *Thin Solid Films* **2007**, 515, 5997- 5999.
- 10 Katagiri, H.; Jimbo, K.; Yamada, S.; Kamimura, T.; Maw, W. S.; Fukano, T.; Ito, T.; Motohiro, T. *Appl. Phys. Express* **2008**, 1, 041201-2.
- 11 Katagiri, H.; Jimbo, K.; Maw, W. S.; Oishi, K.; Yamazaki, M.; Araki, H.; Takeuchi, A. *Thin Solid Films* **2009**, 517, 2455- 2460.
- 12 Shin, B.; Gunawan, O.; Zhu, Y.; Bojarczuk, N. A.; Chey, S. J.; Guha, S. *Prog. Photovoltaics: Research and Applications* **2013**, 21, 72- 76.
- 13 Scragg, J. J.; Berg, D. M.; Dale, P. J. *J. Electroanal. Chem.* **2010**, 646, 52- 59.
- 14 Kumar, Y. B. K.; Babu, G. S.; Bhaskar, P. U.; Raja, V. S. *Sol. Energ. Mater. Sol. Cells* **2009**, 93, 1230- 1237.
- 15 Zeng, X.; Tai, K. F.; Zhang, T.; Ho, C. W. J.; Chen, X., Huan, A.; Sum, T. C.; Wong, L. H. *Sol. Energ. Mater. Sol. Cells* **2014**, 124, 55- 60.
- 16 Guo, Q.; Ford, G. M.; Yang, W. C.; Walker, B. C.; Stach, E. A.; Hillhouse, H. W.; Agrawal, R. *J. Am. Chem. Soc.* **2010**, 132, 17384- 17386.

- 17 Winkler, M. T.; Wang, W.; Gunawan, O.; Hovel, H. J.; Todorov, T. K.; Mitzi, D. B. *Energ. Environ. Sci.* **2014**, 7, 1029-1036.
- 18 Guo, Q.; Hillhouse, H. W.; Agrawal, R. *J. Am. Chem. Soc.* **2009**, 131, 11672- 11673.
- 19 Riha, S. C.; Parkinson, B. A.; Prieto, A. L. *J. Am. Chem. Soc.* **2009**, 131, 12054-12055.
- 20 Suehiro, S.; Horita, K.; Kumamoto, K.; Yuasa, M.; Tanaka, T.; Fujita, K.; Shimanoe, K.; Kida, T. *J. Phys. Chem. C* **2013**, 118, 804-810.
- 21 Gao, Y.; Yang, H.; Zhang, Y.; Li, J.; Zhao, H.; Feng, J.; Sun, J.; Zheng, Z. *RSC Adv* **2014**, 4, 17667 -17670.
- 22 Chesman, A. S. R.; Duffy, N. W.; Peacock, S.; Waddington, L.; Webster, N. A. S., Jasieniak, J. J. *RSC Adv.*, **2013**, 3, 1017-1020.
- 23 Todorov, T. K.; Reuter, K. B.; Mitzi, D. B. *Adv. Mater.* **2010**, 22, E156- E159.
- 24 Kumar, Y. B. K.; Bhaskar, P. U.; Babu, G. S.; Raja, V. S. *Phys. Status Solidi A* **2010**, 207, 149-156.
- 25 Kumar, Y. B. K.; Babu, G. S.; Bhaskar, P. U.; Raja, V. S. *Phys. Status Solidi A* **2009**, 206, 1525-1530.
- 26 Cao, Y.; Denny, M. S.; Caspar, J. V.; Farneth, W. E.; Guo, Q.; Lonkin, A. S.; Johnson, L. K.; Lu, M.; Malajovich, I.; Radu, D.; Rosenfeld, H. D.; Choudhury, K. R.; Wu, W. *J. Am. Chem. Soc.* **2012**, 134, 15644- 15647.
- 27 Woo, K.; Kim, Y.; Moon, J. *Energy Environ. Sci.* **2012**, 5, 5340- 5345.
- 28 Cheng, J.; Manno, M.; Khare, A.; Leighton, C.; Campbell, S. A.; Aydil, E. S. *J. Vac. Sci. Technol. A* **2011**, 29, 051203-2.
- 29 Fernandes, P. A.; Salomé, P. M. P.; da Cunha, A. F. *Thin Solid Films* **2009**, 517, 2519- 2523.
- 30 Altosaar, M., Raudoja, J.; Timmo, K.; Danilson, M.; Grossberg, M.; Krustok, J.; Mellikov, E. *Phys. Status Solidi A* **2008**, 205, 167- 170.

- 31 Munce, G.; Parker, G. K.; Holt, S. A.; Hope, G. A. *Colloid. Surface. A* **2007**, 295, 152- 158.
- 32 Cheng, Y. C.; Jin, C. Q.; Gao, F.; Wu, X. L.; Zhong, W.; Li, S. H.; Chu, P. K. *J. Appl. Phys.* **2009**, 106, 123505-5.
- 33 Adelifard, M.; Mohagheghi, M. M. B.; Eshghi, H. *Phys. Scr.* **2012**, 85, 035603-035608.
- 34 Sarswat, P. K.; Free, M. L.; Tiwari, A. *Phys. Status Solid B* **2011**, 248, 2170- 2174.
- 35 Weber, A.; Mainz, R.; Schock, H. W. *J. Appl. Phys.* **2010**, 107, 013516-2.
- 36 Haight, R.; Barkhouse, A.; Gunawan, O.; Shin, B.; Copel, M.; Hopstaken, M. *App. Phy. Lett.* **2011**, 98, 253502 -3.
- 37 Riha, S. C.; Parkinson, B. A.; Prieto, A. L. *J. Am. Chem. Soc.* **2011**, 133, 15272 - 15275.

Figure Captions

Fig. 1. Experimental method for preparation of CZTS thin films using CuS, ZnS and SnS₂ nanoparticles.

Fig. 2. Bright-field TEM images of the as-synthesized nanoparticles: (a) CuS, (b) ZnS and (c) SnS₂. The TEM samples were prepared by drop-casting the respective binary sulfide nanoparticles dispersed in ethanol onto carbon-coated copper TEM grids (200 mesh, Ted Pella).

Fig. 3. XRD patterns from the as-prepared precursor film and films after annealing at 200, 300, 400 and 450 °C. Reference diffraction peaks for kesterite CZTS (JCPDS no. 26-0575) are displayed at the bottom.

Fig. 4. Raman spectra from the films annealed at 300, 400 and 450 °C. The peak position of the 288, 336 and 368 cm⁻¹ lines are marked with vertical dotted lines.

Fig. 5. Scanning electron micrographs from the sample annealed at 400 °C. (a) Plan view and (b) cross-sectional view of the as-prepared CZTS thin film.

Fig. 6. (a) XRD patterns from a CZTS film prepared by annealing the precursor film at 500°C and from a CZTSSe film prepared by selenizing the precursor film. (b) Enlargement of the 112 reflection.

Fig. 7. (a) Cross-sectional SEM image of the CZTSSe thin film solar cell and (b) J-V curve from the as-prepared CZTSSe solar cells in dark and under AM1.5G illumination.

Fig. 8. (a) External quantum efficiency (EQE) curve from the CZTSSe solar cell. The inset shows a corresponding $(E \ln(1-EQE))^2$ vs. $h\nu$ plot where the band gap of the absorber is determined to be 1.18 eV.

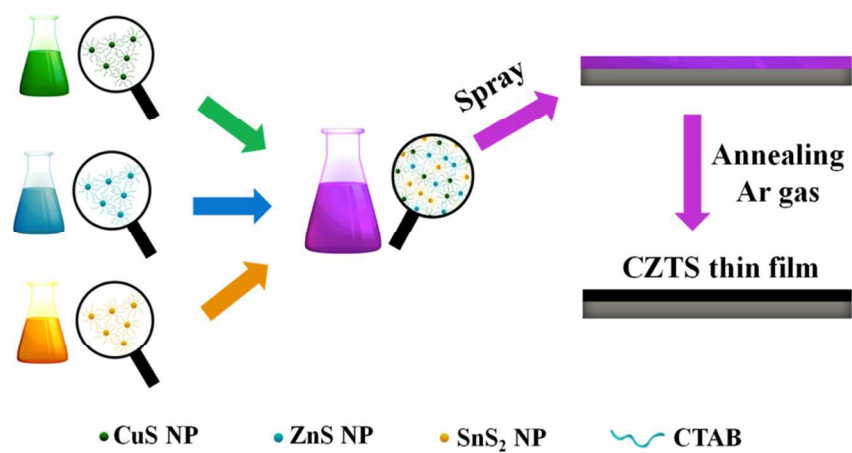


Fig. 1 Experimental method for preparation of CZTS thin films using CuS, ZnS and SnS₂ nanoparticles.

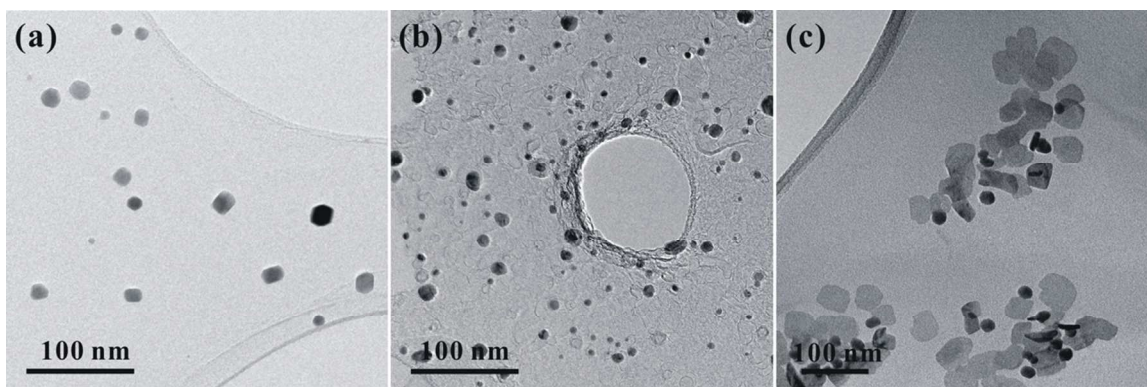


Fig. 2. Bright-field TEM images of the as-synthesized nanoparticles: (a) CuS, (b) ZnS and (c) SnS₂. The TEM samples were prepared by drop-casting the respective binary sulfide nanoparticles dispersed in ethanol onto carbon-coated copper TEM grids (200 mesh, Ted Pella).

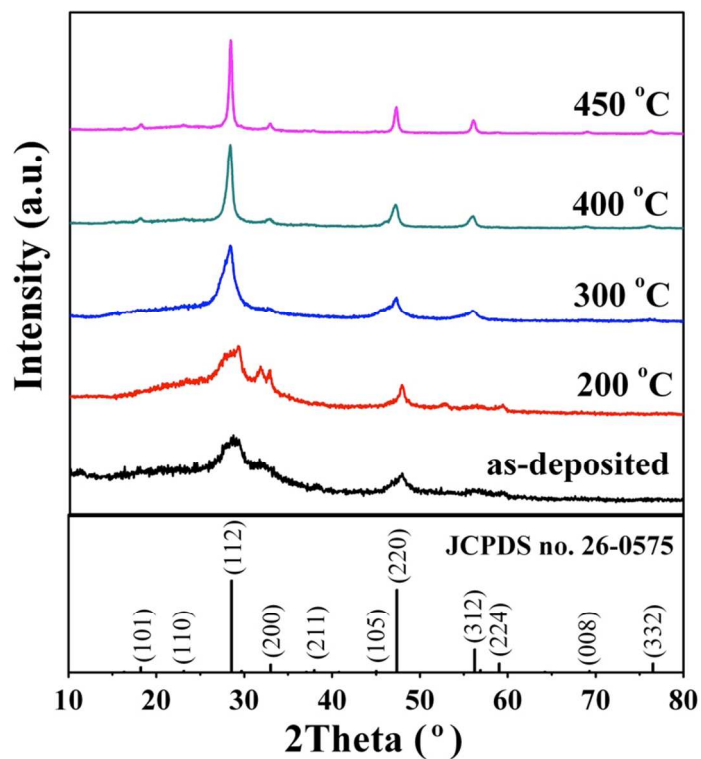


Fig. 3. XRD patterns from the as-prepared precursor film and films after annealing at 200, 300, 400 and 450 °C. Reference diffraction peaks for kesterite CZTS (JCPDS no. 26-0575) are displayed at the bottom.

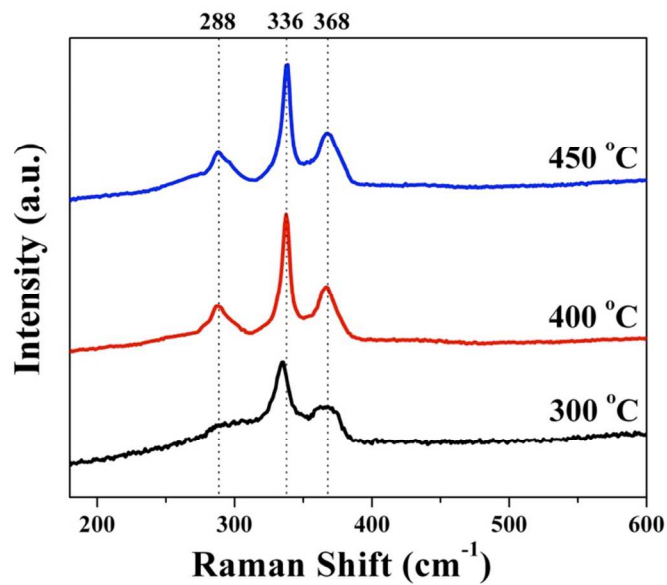


Fig. 4. Raman spectra from the films annealed at 300, 400 and 450 °C. The peak position of the 288, 336 and 368 cm^{-1} lines are marked with vertical dotted lines.

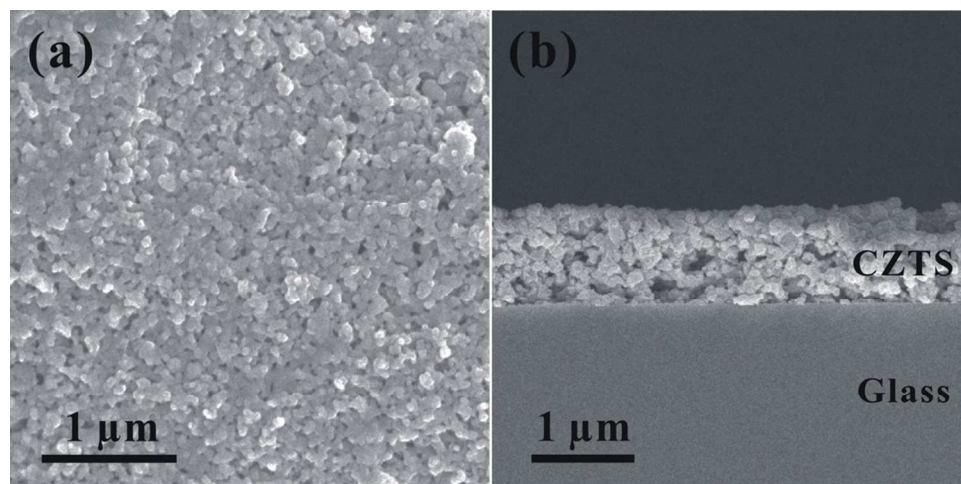


Fig. 5. Scanning electron micrographs from the sample annealed at 400 °C. (a) Plan view and (b) cross-sectional view of the as-prepared CZTS thin film.

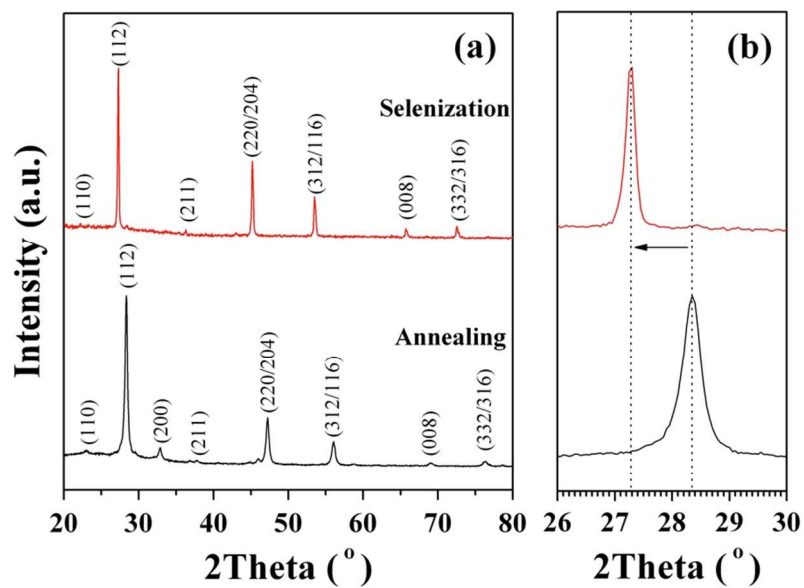


Fig. 6. (a) XRD patterns from a CZTS film prepared by annealing the precursor film at 500°C and from a CZTSSe film prepared by selenizing the precursor film. (b) Enlargement of the 112 reflection.

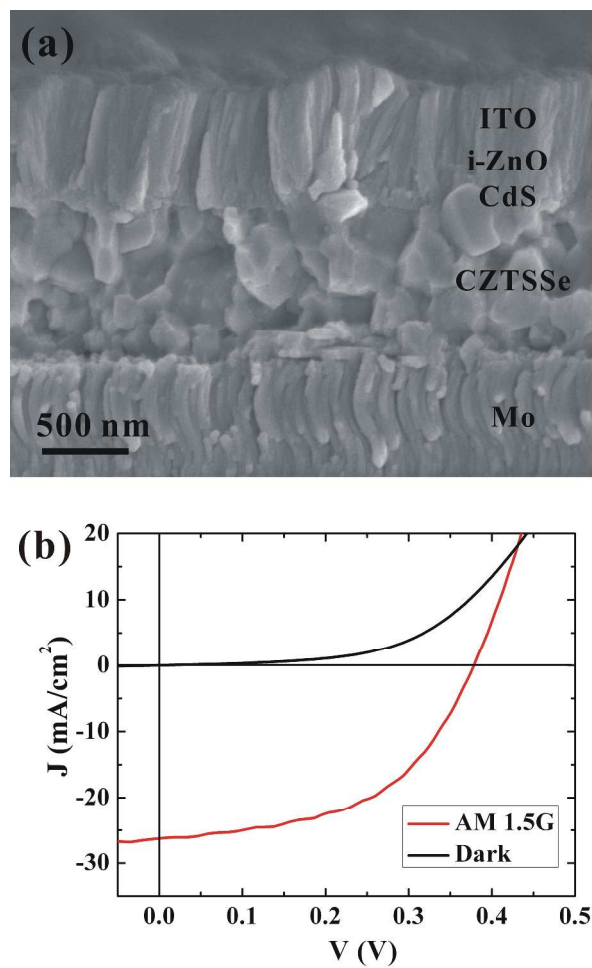


Fig. 7. (a) Cross-sectional SEM image of the CZTSSe thin film solar cell and (b) J-V curve from the as-prepared CZTSSe solar cells in dark and under AM1.5G illumination.

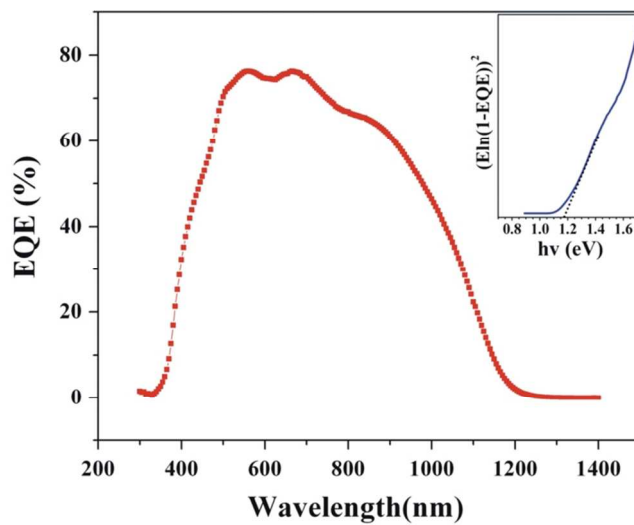
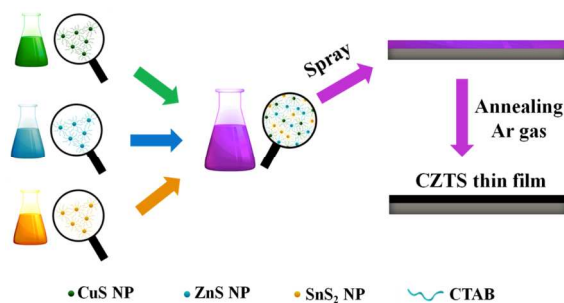


Fig. 8. (a) External quantum efficiency (EQE) curve from the CZTSSe solar cell. The inset shows a corresponding $(E \ln(1-EQE))^2$ vs. $h\nu$ plot where the band gap of the absorber is determined to be 1.18 eV.

Environmentally friendly solution route to kesterite $\text{Cu}_2\text{ZnSn}(\text{S,Se})_4$ thin films for solar cell applications

Zhenggang Li, John C. W. Ho, Kian Keat Lee, Xin Zeng, Tianliang Zhang, Lydia Helena Wong, Yeng Ming Lam



Highlight

Solar cells were made from $\text{Cu}_2\text{ZnSn}(\text{S,Se})_4$ thin films prepared using an ink consisting of CuS, ZnS and SnS₂ nanoparticles dispersed in water.